Remote Sensing of Environment 235 (2019) 111432

Contents lists available at ScienceDirect

Remote Sensing of Environment

journal homepage: www.elsevier.com/locate/rse

Lidar provides novel insights into the effect of pixel size and grazing intensity on measures of spatial heterogeneity in a native bunchgrass ecosystem

By V.S. Jansen[a,*], C.A. Kolden[a], H.E. Greaves[b], J.U.H. Eitel[c,d]

[a] Department of Forest, Rangeland and Fire Sciences, College of Natural Resources, University of Idaho, Moscow, ID, 83844-1133, USA
[b] Institute of Arctic Biology, University of Alaska Fairbanks, Fairbanks, AK, 99775-7000, USA
[c] Department of Natural Resources and Society, University of Idaho, College of Natural Resources, Moscow, 83844-1133, USA
[d] McCall Outdoor Science School, University of Idaho, McCall, ID, 83638, USA

ARTICLE INFO

Keywords:
Lidar
Spatial heterogeneity
Semivariograms
Grasslands
Grazing
Aboveground biomass

ABSTRACT

There is a strong link between vegetation heterogeneity and biodiversity in grassland ecosystems. However, quantifying spatial patterns of key metrics, such as aboveground biomass, at landscape scales remains a challenge. This stems from difficulties in accurately estimating grassland biomass at fine scales over large areas and determining what spatial scale is most appropriate to monitor how grassland impacts (e.g., livestock grazing) affect spatial patterns of biomass (i.e., spatial heterogeneity). Here, we use lidar metrics (volume, max height, and intensity) in Random Forest models to quantify fine-resolution (pixel size 1.0668 m (3.5 ft)) aboveground biomass estimates (pseudo R^2 = 0.59; RMSD = 139.4 g m^{-2}) across a bunchgrass prairie grassland system. To determine both the effects of grazing on the spatial heterogeneity of aboveground biomass and which pixel size is most sensitive to the effects of livestock grazing on grassland heterogeneity, we aggregated fine-resolution biomass maps to coarser pixel resolutions (3 m, 5 m, 8 m, 20 m, 30 m) across 23 pastures with varying levels of grazing intensity. Following aggregation to coarser pixel resolutions, we observed that semivariogram models produced statistically different (α = 0.05) measures of biomass heterogeneity. The range statistic was the only pasture-level semivariogram metric sensitive to grazing, and this relationship was only significant when using the finer-resolution datasets (~1 m to 8 m pixels). Our results demonstrate 1) the applicability of lidar data for quantifying biomass in short-statured grasslands, 2) that grazing in pacific northwest bunchgrass prairie can decrease spatial heterogeneity of aboveground biomass and 3) that fine-resolution satellite data (< 10 m pixel sizes) are necessary to effectively monitor the effects of grazing on the spatial heterogeneity of vegetation biomass, an indirect metric of biodiversity at management scales (pasture sizes ranged from 40 to 745 ha) in this grassland ecosystem.

1. Introduction

Natural grassland ecosystems are subject to drivers of environmental change such as grazing and drought, which impact the conservation of critical species (Fleischner, 1994), annual forage production (Augustine and McNaughton, 1998), proper ecosystem function (Allen-Diaz et al., 1995), and carbon storage (McSherry and Ritchie, 2013). However, relationships and feedbacks between drivers and outcomes of interest are relatively poorly understood (Herrick et al., 2010). Land managers interested in monitoring grassland system responses to environmental drivers have called for more research to study vegetation patterns and processes at larger spatial and temporal scales that align with land management practices (Bestelmeyer and Briske, 2012; Sayre et al., 2013, 2012). This is due, in part, to the increasing need to quantify and monitor ecosystem services beyond livestock forage, and promote processes that increase vegetation heterogeneity given its positive link to biological diversity (Adler et al., 2001; Fuhlendorf & Engle, David, 2001; Fuhlendorf et al., 2012). Management practices such as grazing can have positive or negative impacts on various parameters of vegetation heterogeneity such as species composition, structure and biomass (Adler et al., 2001; Fuhlendorf and Engle, David, 2001; Hempson et al., 2015), but few grassland studies quantify the effect of grazing on vegetation heterogeneity spatially using any of the above parameters (Adler et al., 2001; Bestelmeyer and

* Corresponding author.
E-mail address: vjansen@uidaho.edu (B.V.S. Jansen).

https://doi.org/10.1016/j.rse.2019.111432
Received 6 March 2019; Received in revised form 20 August 2019; Accepted 17 September 2019
Available online 24 October 2019

Briske, 2012) and fewer still quantify vegetation heterogeneity spatially using remotely sensed data (e.g. Virk and Mitchell, 2015).

We focus on quantifying the spatial heterogeneity of aboveground biomass, because in grassland systems biomass amount is a commonly used indicator to assess and plan grazing management (Benkobi et al., 2000; Friedel et al., 1988), and is correlated to measures of vegetation structure (e.g. Heady, 1957; Robel et al., 1970). To quantify spatial heterogeneity of vegetation biomass and how this pattern is impacted by grazing, two issues need to be addressed initially: 1) quantifying biomass accurately across the landscape and 2) determining the spatial resolution at which to quantify heterogeneity which is most sensitive to the grazing process. Using field plot measures to accurately assess grassland vegetation metrics at landscape scales has proven difficult (Booth and Tueller, 2003; Pickup et al., 1994; West, 2003). The cost, time, and observer bias associated with field data collection and the need to monitor vegetation across large areas has led land managers and scientists to turn to remotely sensed data to provide estimates of grassland metrics such as cover or biomass (Booth and Tueller, 2003; Guerschman et al., 2015) as well as biodiversity (Turner et al., 2003; Wang and Gamon, 2019). While a variety of remotely sensed datasets and analysis methodologies have focused on providing measures of grassland biomass (Anderson et al., 1993; Friedl et al., 1994; Jacques et al., 2014; Jansen et al., 2018; Marsett et al., 2006; Todd et al., 1998), and more recently estimates of species diversity (Gholizadeh et al., 2019), providing spatial measures of vegetation heterogeneity with gridded remotely sensed data is challenging, due to the interaction between the scale of the imagery and the underlying physical or biologic pattern in question (Karl and Maurer, 2010). The ability to quantify patterns that are used to infer how an ecological process is impacting the landscape is tied to the grain size and extent of the study (Wiens, 1989). These relationships in turn impact the choice of spatial resolution (i.e. pixel size) to use for analysis, as well as the analysis results (Hudak and Wessman, 1998; Lechner et al., 2009; Woodcock and Strahler, 1987).

Similarly, there is a need to identify what metric of spatial heterogeneity is appropriate to the ecological process of interest. Spatial heterogeneity can be quantified using a variety of metrics, including non-spatially dependent measures like the coefficient of variation, which provides a measure of variability over an area or distance (Adler et al., 2001), and spatially dependent measures produced using categorical maps, such as fractals, contagion, evenness, and patchiness (Li and Reynolds, 1994). Geo- or spatial-statistics provide another way to quantify spatial heterogeneity in continuous numerical data, producing measures of spatial dependence and spatial pattern (Adler et al., 2001). Spatial statistics such as Moran's I (Moran, 1950), the Getis-Ord general G statistic (Getis and Ord, 1992), semivariograms and correlograms have all been used to provide spatial metrics of gridded remotely sensed data and to explore how grazing affects vegetation heterogeneity (e.g Virk and Mitchell, 2015; Sankey et al., 2009). In this study, we focus on measures of spatial heterogeneity that quantify spatial patterns of continuous numerical data, as found in remotely sensed imagery.

Landscape-scale studies using remotely sensed data to quantify grassland spatial heterogeneity in relation to grazing have been conducted primarily with moderate-resolution passive sensors, including 10 m Sentinel-2 data (Scarth and Trevithick, 2017), 30 m Landsat data (Virk and Mitchell, 2015), and 20 m data from Satellite Pour l'Observation de la Terre (SPOT) (Sankey et al., 2009). These previous studies provide spatial heterogeneity metrics for their respective ecosystems, but they do not explore the sensitivity of the reported spatial heterogeneity to the spatial resolution of the remotely sensed data to help guide the selection of the most appropriate scale to monitor the grazing process. They are also limited by the use of passive satellite sensors, which lack the ability to directly quantify vegetation structure or height. In contrast to passive satellite sensors, active sensors such as lidar can more accurately assess vegetation structure, types, and biomass by providing 3-dimensional data as well as return intensity data on vegetation and surfaces (Eitel et al., 2016a; Hudak et al., 2009). While passive structure-from-motion photogrammetry techniques can also generate 3-dimensional point clouds to estimate grassland biomass (Wijesingha et al., 2019) or structure (Forsmoo et al., 2018), currently this technique is applied to smaller extents or plots (< 1 ha) within fields or pastures (e.g. (Gillan et al., 2019; Wijesingha et al., 2019) not multiple complete pasture areas.

Lidar in comparison can map larger spatial extents and is commonly used to map forested ecosystems, and is increasingly being used to map small-statured vegetation communities such as arctic tundra (Greaves et al., 2016), salt marsh habitat (Kulawardhana et al., 2014), and the sage-brush steppe (Glenn et al., 2015; Li et al., 2017) yet research to-date in grassland systems is limited. This is potentially due to known limitations of lidar when estimating small-statured vegetation metrics, such as the negative impact of dense vegetation on lidar pulse penetration to the soil surface (Kulawardhana et al., 2014), or missing the highest portion of the plant material due to the sampling density and laser spot size of the lidar point cloud (Greaves et al., 2016).

Recent research suggests that despite these limitations, structural vegetation metrics such as biomass and height can be reliably measured with lidar in low-stature ecosystems (Greaves et al., 2016, 2015; Kulawardhana et al., 2014). Within grassland systems, vegetation metrics at plot scales have been quantified using ground-based terrestrial laser scanners (TLS) (Cooper et al., 2017; Eitel et al., 2014) or vehicle-mounted lidar systems (Radtke et al., 2010; Schaefer and Lamb, 2016). Discrete return lidar collected with an unmanned aerial vehicle (UAV) has also demonstrated statistically significant relationships between lidar metrics and field estimates of canopy heights, cover and biomass in grasslands (Wang et al., 2017). Full waveform lidar collected by airplane during leaf-on and leaf-off dates has been used to classify grassland habitat (Zlinszky et al., 2014), as well as to provide information for conservation objectives (Zlinszky et al., 2015), but rarely has airborne lidar been used to quantify biomass and vertical structure in natural grassland systems.

Because lidar can provide accurate fine-scale measures of vegetation biomass or structure, it can also facilitate an exploration of how grain size (i.e. the pixel size of imagery) impacts the quantification of vegetation heterogeneity, as the raw point cloud data can be aggregated to increasingly coarser pixel sizes (Eitel et al., 2016b). It is ideal for remote sensing and ecological studies to quantify phenomena across varying grain sizes and spatial extents to provide a more complete understanding of how the process and pattern is impacted by the scales chosen for inquiry (e.g. Hudak and Wessman, 1998; Woodcock and Strahler, 1987), but cost, logistics and technology are often real-world barriers. The selection of remotely sensed data for analysis should be based on knowledge of the system (i.e., the scene model; Woodcock and Strahler, 1987), cost, the objectives of the study, and the scale at which subsequent management action happens (Phinn et al., 2003; Wiens et al., 2009). The underlying assumption in selecting one pixel size or sensor to quantify spatial heterogeneity is that the resolution of the spectral data is finer than or equal to the scale of the heterogeneity of the ecological object or pattern in question; however, in most cases the ideal spatial resolution (i.e. pixel size) is unknown (Johansen et al., 2007). While airborne lidar datasets are too costly for monitoring grassland biomass or heterogeneity with repeat acquisitions, they can be used to assess the pixel size at which critical patterns of spatial heterogeneity are no longer detectable, thus answering the question of whether more affordable (but coarser-resolution) passive reflectance sensors can accurately quantify patterns of spatial heterogeneity in grassland biomes.

Our research objectives for this study were to 1) accurately model bunchgrass vegetation biomass from airborne lidar data using vegetation canopy, intensity and topographic metrics, 2) determine the impact of decreasing spatial resolution (i.e., increasing grain size) on measures of spatial heterogeneity, and 3) identify the measures of spatial heterogeneity most sensitive to grazing intensity and how this sensitivity

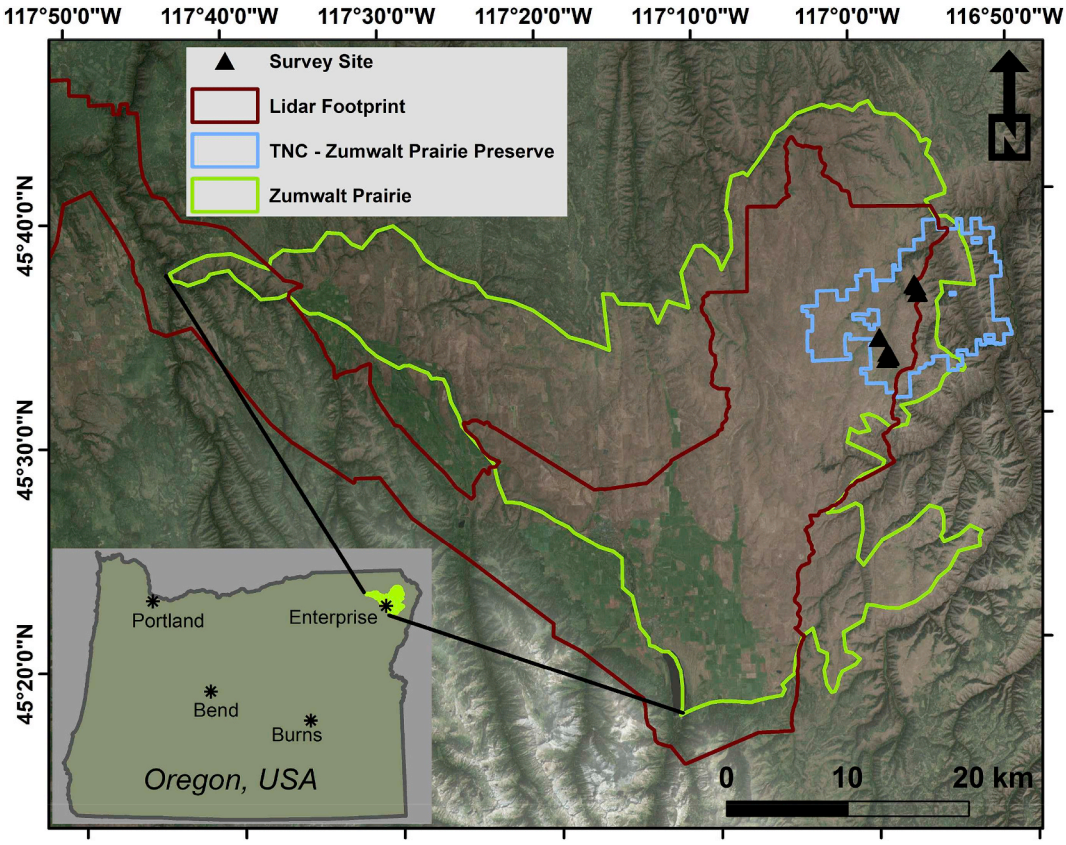

Fig. 1. Map of the Zumwalt Prairie study area showing the intersection between the lidar footprint, the Zumwalt Prairie grassland habitat, and the Zumwalt Prairie Preserve (TNC). Locations where field data were collected are shown with black triangles. Because the majority of the Zumwalt Prairie is privately owned, our sample locations were limited to The Nature Conservancy (TNC) Zumwalt Prairie Preserve boundaries.

changes with increasing spatial resolution of remotely sensed data.

2. Methods

2.1. Study area

The Zumwalt Prairie is a Pacific Northwest Bunchgrass Prairie (PNWBP) habitat located in northeast Oregon (Fig. 1). The PNWBP is a highly threatened and understudied temperate grassland ecosystem (Kimoto et al., 2012; Tisdale, 1982) dominated by C3 bunchgrass species, including Idaho fescue (*Festuca idahoensis* Elmer), bluebunch wheatgrass (*Pseudoroegneria spicata* (Pursh) A. Love) and Sandberg's bluegrass (*Poa secunda* J Presl) which may be especially vulnerable to harmful effects of poorly managed grazing compared to other grassland systems (Adler et al., 2004; Mack and Pyke, 1983; McLean and Tisdale, 1972). Elevations across the study area range from 1000 m to 1600 m. Average summer (June–August) temperatures range from 11.8 – 17.5 °C, with average annual precipitation of 348.3 mm (2006–2012 Zumwalt Weather Station).

2.2. Data

2.2.1. Vegetation field data

The Oregon Department of Geology and Mineral Industries (DOGAMI) contracted a lidar acquisition flight over the study area as part of a statewide collection effort in 2015 (section 2.2.3). In conjunction, we collected data on aboveground vegetation biomass, height, and foliar cover within 65 1 m^2-quadrats on The Nature Conservancy's Zumwalt Prairie Preserve property 10–14 July 2015, directly after the lidar flight. This sampling period was selected to correspond with peak biomass and a time when most of the perennial grasses and forbs are still photosynthetically active. Quadrat locations were subjectively selected in the field to represent a gradient of vegetation biomass (e.g. Greaves et al., 2016) from quadrats containing no vegetation (i.e., bare ground) to quadrats dominated by Basin Wildrye (*Leymus cinereus* (Scribn. & Merr) A. Love), a bunchgrass species which typically has the largest vegetative growth (in both structure and biomass) compared to the other common bunchgrass species found within the study area (See Table S1 for quadrat photos). Vegetation cover and height data were estimated across 36 evenly distributed points within each 1 m^2-quadrat using a grid-point intercept approach following Godínez-Alvarez et al. (2009). Biomass data were collected by harvesting all standing vegetation within the quadrat. All clipped vegetation was bagged in the field and oven dried at 60 °C to obtain a dry weight for analysis. The center XY location of each quadrat was obtained using a TopCon GR-3 survey grade GPS system (nominal horizontal accuracy ~4 cm) running in Real Time Kinematic (RTK) mode using the same vertical and horizontal datum as the airborne lidar data.

2.2.2. Grazing management data

We obtained stocking rate data from the land managers for each pasture area within the study area. Stocking rates by pasture are expressed as Animal Unit Months per hectare (AUM ha^{-1}). Adjustments in the stocking rates were calculated using animal use equivalencies (AUE) for the different type of livestock type (e.g. bulls had 1.2 AUE, yearlings 0.75 AUE, and cow-calf pairs 1.0 AUE). For subsequent analysis we selected pastures across the study site that consisted primarily of upland prairie grassland habitat and were grazed in 2015 before the lidar flight or were un-grazed for more than two years prior to the lidar acquisition. These selection criteria produced 23 unique pastures that averaged 125 ha (range 40 ha to 745 ha) for further analysis, eight of which had no recorded livestock grazing and 15 that had an average

stocking rate of 0.80 Animal Unit Months per Hectare (AUMs/ha), and a range of 0.39–1.718 AUMs/ha. To minimize the impact of non-grassland habitat and other objects on our results, we masked out the non-grassland habitat, human-made structures, and stock ponds, and buffered all fences and roads across the analyzed pastures.

2.2.3. Lidar data

Airborne lidar data were collected by Quantum Spatial on July 4th - July 10th, 2015 using a Leica ALS70. The Lecia ALS70 uses a near infrared (1064 nm) laser with a beam divergence of 0.15 mrad. The discrete return lidar dataset averaged 9.29 points per square meter with a fundamental non-vegetated vertical precision of 3.7 cm, vertical bias of −1.3 cm, a horizontal accuracy of 5.4 cm, and an average pulse footprint diameter of 32 cm, with a 1400 m survey altitude and a field of view ± 14° from nadir (Quantum Spatial Technical Report). The vendor provided point and laser return intensity raster data in the Oregon Statewide Lambert projection with a horizontal datum of NAD83 (2011) and a vertical datum NAVD88 (Geoid12A). We processed the lidar data in its native projection to match the vendor data and end user needs. There was high variability in pulse densities at the 1 m scale across the study area which biased the data (Fig. S1); therefore, we resampled the point cloud to create an even point density for biomass mapping using CloudCompare software (CloudCompare v2.6.2 2017). To do this, we fit a Delaunay 2.5D best fitting plane to the vendor-provided point data, then sampled this plane to the chosen density of 0.85 points per square foot (9.15 points per square meter). This step was performed because initial analysis using the raw lidar point clouds produced maps with notable striping (see discussion for more detail, and Fig. S1).

2.3. Modeling bunchgrass biomass with lidar data

2.3.1. Variable creation from lidar data

2.3.1.1. Lidar-derived volume metric. Following Greaves et al. (2015) and (2016), we created a canopy volume raster using an optimization algorithm that produces a set of gridded ground and canopy surfaces based on user-defined parameters (Eitel et al., 2014; Greaves et al., 2015). We aggregated the canopy volume raster data to 1.0668 m (3.5 ft) maintaining the imperial state plane units corresponding to the vendors units and the end-users' needs, and to minimize the errors introduced by projecting raster data between datums (For more detailed information on the creation of the volume metric, see supplementary text 1).

2.3.1.2. Canopy lidar metrics. Using the ground points generated during creation of the canopy volume metric, we normalized the point cloud to compute a set of common lidar metrics at the 1.0668 m (3.5 ft) scale. Using all the points greater than 2 cm height we computed the minimum, maximum, mean, standard deviation, and 25th and 75th percentiles of heights. We also computed total return and canopy density (Table 1).

2.3.1.3. Intensity data. Zonal means of the vendor-provided 0.3048 m (1 ft) intensity data were computed for each 1 m^2 field vegetation quadrat. We computed the mean and max intensity for each of the 65 quadrats (Table 1, dataset: Intensity). The vendor performed minimal normalization accounting for the pulse distance, angle and channel-balancing using a propriety approach (pers. comm. with Quantum Spatial).

2.3.1.4. Lidar derived topographic metrics. Using the ground surface rasters obtained from the canopy volume creation, we created several topographic metrics at the 1.0668 m scale, including slope, aspect, curvature and the SAGA wetness index (Boehner et al., 2002) (Table 1). These variables, associated with topography, were included due to their potential influence on soil moisture, vegetation production (Gessler et al., 2000) and vegetation type (Fu et al., 2004) (Table 1, dataset: Topographic).

Table 1
Lidar-derived variables used to model aboveground biomass.

Data Type	Variable	Details
Canopy	Vol	Canopy volume (Greaves et al., 2015, 2016)
Canopy	H_Mean	Average height
Canopy	H_Std	Standard deviation of height
Canopy	H_Max	Max height
Canopy	Tot_Returns	Number of all lidar returns
Canopy	Canopy_Dns	Points above 2 cm divided by all returns
Intensity	Int_Mean	Mean of vendor 0.3048 cm (1 ft) intensity raster
Intensity	Int_Max	Max of vendor 0.3048 cm (1 ft) intensity raster
Topographic	SWI	Saga Wetness Index SAGA GIS
Topographic	Slope	ArcMap Spatial Analyst Package
Topographic	Aspect	ArcMap Spatial Analyst Package
Topographic	Curve	ArcMap Spatial Analyst Package

2.3.2. Model creation using Random Forests

Following methods described in Greaves et al. (2016), we used Random Forests (Breiman, 2001) implemented in the randomForest package (Liaw and Wiener, 2002) in R (R Development Core Team, 2016) to determine what predictors most accurately estimated biomass. When run in regression mode, Random Forest provides model estimates by averaging the predictions across many decision trees, which are constructed based on a random selection of the input data, as well as a random selection of the predictor variable used at each splitting node (Breiman, 2001). We tested seven different predictor sets to model biomass: 1) canopy, 2) topography (topo), 3) intensity, 4) canopy + topo, 5) canopy + intensity, 6) intensity + topo, and 7) canopy + intensity + topo. To reduce the possibility of overfitting the models, for each predictor set we removed the highly correlated predictor variables (Spearman's rank r > 0.90). To further limit the predictor variables within each of the seven sets of predictor sets, we ran the model selection tool in the rfutilities package (Murphy et al., 2010) 1000 times and only included the variables which were selected in the majority (i.e. greater than 500) of model runs for subsequent Random Forest modelling. The best Random Forest models generated from each predictor set were then compared using the Random Forest pseudo R^2, as well as the r-squared values between the predicted and observed estimates and the associated root mean squared difference (RMSD) (Pineiro et al., 2008) metrics of the out-of-bag training samples.

2.3.3. Biomass mapping and summary statistics at the pasture scale

Using the Random Forest model that minimized the RMSD, we employed the AsciiGridPredict Tool in the R package 'yaImpute' (Crookston and Finley, 2008) to predict biomass at 1.0668 m pixel resolution across the study area. For each pasture across the study area that met our selection criteria (see section 2.2.2) we computed summary statistics for biomass within each pasture, including the mean, the 10th, 25th, 50th, 75th, and 90th percentiles, the standard deviation, and the coefficient of variation (CV).

2.4. The effect of spatial resolution on measures of heterogeneity

2.4.1. Upscaling the 1.0668 m biomass data to coarser scales

To provide biomass estimates at varying resolutions, we aggregated the 1.0668 m masked biomass rasters for each pasture area to coarser spatial resolutions: 3 m, 5 m, 8 m, 20 m, and 30 m pixel sizes. We kept the geographic extent of the analysis areas fixed and consistent with the pasture areas, as this is the size related to grazing management. To do this, we re-projected the 1.0668 m biomass data from the NAD1983 2011 Oregon Statewide Lambert International Feet to WGS1984 UTM Zone 11. Next, we resampled the 1.0668 m data to 1 m using the bilinear approach and then aggregated by averaging the 1 m data to the

Table 2
Summary statistics for field biomass (g/m2) and vegetation height (cm) data (N = 65).

Field Metric	Mean	Min	Max	10th percentile	90th percentile	SD
Aboveground Biomass (g/m^2)	268.9	0.0	1213.9	24.7	467.5	262.3
Mean Height (cm)	12.9	0.0	45.5	3.1	20.8	9.6
Max Height (cm)	29.5	0.0	91.0	6.0	45.4	20.3

five coarser spatial resolutions. The coarser-scale spatial resolutions (pixel sizes) were selected to align with currently available short-wave infrared data from satellites such as WorldView-3 (4 to 8 m), Sentinel-2 (20 m), and Landsat (30 m) because of the importance of these wavebands in quantifying grassland vegetation in this system (Jansen et al., 2018, 2016).

2.4.2. Variogram stats

The biomass raster data for each pasture and pixel resolution were used to compute semivariograms to explore spatial measures of heterogeneity. The computation of the semivariogram takes the form:

$$\gamma(h) = \frac{1}{2n}\sum_{i=1}^{n}\left|z(s_i) - z(s_{i+h})\right|^2$$

where $\gamma(h)$ is the semivariance for the distance bin h, z is the value of the biomass variable at two locations s_i *and* s_{i+h}, with h signifying the distance between each pair and n is the number of pairs of sampling locations across each lag (or bin) h. For each pasture area we fit theoretical models consisting of the exponential, spherical, and linear form to the empirical semivariogram using the GSTAT package (Pebesma, 2004). We used the output from the exponential models for subsequent analysis, as these decreased errors across the majority of pastures and resolutions. From the theoretical semivariograms the sill, nugget, and range were computed. The sill refers to the point at which the variance no longer increases with increasing lag distances (variance beyond the range); the range is a measure of spatial dependence across distance, signifying the distance at which the variable in question is no longer autocorrelated, and provides an indicator of patch size (Townsend and Fuhlendorf, 2010). The nugget is the intercept along the y-axis representing variability or sampling error within the zero lag distance (Fortin and Dale, 2005; Sadoti et al., 2014; Townsend and Fuhlendorf, 2010; Western et al., 1998). From the sill, nugget, and range metrics we calculated the magnitude of spatial heterogeneity (MSH) (Lane and BassiriRad, 2005; Lin et al., 2010). The MSH is calculated by dividing the spatially structured variation (the sill minus the nugget) by the total sample variation (the sill) (Lane and BassiriRad, 2005) and ranges from 0-1, with zero indicating no spatially structured heterogeneity and one indicating highly structured heterogeneity (Virk and Mitchell, 2015). We also calculated the nugget to sill ratio: (nugget semivariance/total semivariance)*100 (Cambardella et al., 1994).

2.4.3. The effect of spatial resolution on measures of heterogeneity

To visualize how varying resolutions (pixel size) influenced the measures of spatial heterogeneity (i.e. sill, nugget, range, etc.), we created boxplots for each semivariogram-derived metric by pixel size. To test which resolutions produced significantly different measures of heterogeneity, we computed pairwise Mann-Whitney U rank-sum tests between all possible pairs of pixel sizes. We selected a non-parametric test because many of the semivariogram metrics at the varying pixel sizes did not fit a gaussian distribution. We only performed the multiple comparison Mann-Whitney U tests when the semivariogram-derived metric met the assumption of homogeneity of variance across all groups as tested with the Fligner-Killeen test. Statistically significant p-values were adjusted using the Bonferroni correction.

2.5. The effect of grazing on biomass statistics and measures of heterogeneity across varying resolutions

We explored the effect of grazing on pasture summary statistics and semivariogram-derived measures of heterogeneity using Spearman rank correlations, simple linear models and quadratic models. Because some initial linear models did not have normally distributed residuals, we transformed our predictor variables with log, reciprocal and square root transformations to determine whether these transformations helped in meeting the assumptions of a linear model. The effect of grazing was tested across each of the six resolutions separately and considered significant at $\alpha = 0.05$.

3. Results

3.1. Field measured aboveground biomass and vegetation height data

Across the 65 $1\,m^{-2}$ quadrats sampled in 2015, the average field biomass was $268.9\,g\,m^{-2}$ with a range of $0\,g\,m^{-2}$ to $1213.9\,g\,m^{-2}$ (Table 2). The average mean height was 12.9 cm with a mean height range of 0 cm to 45.5 cm. The average max height across the 65 sites was 29.5 cm and ranged from 0 cm to 91 cm. Spearman rank correlations between biomass and the measures of vegetation structure (height mean and height max) were significant and strongly related ($r^2 > 0.70$) (Fig. 2).

3.2. Modeling grassland biomass with lidar data

3.2.1. Random Forest modeling for aboveground biomass estimates

Using the rfutilites model selection tool to determine what predictors in each predictor set were important (i.e., selected more than 50% of the time across the 1000 runs) revealed that only four of the seven final datasets had a unique set of variables (Table 3). For example, the Canopy + Intensity had the same selected variables as the Canopy + Topo + Intensity, which included volume, max height and mean intensity. The selected predictors from the canopy-only predictor set included the canopy volume metric, max height and canopy density. Slope was the only variable selected in the majority of model runs from the topographic predictor set. For the intensity predictor set, the mean and max intensity metrics were significantly correlated (spearman rank $r > 0.90$), therefore we included only the mean intensity metric for variable selection.

When running Random Forest models across each unique predictor set, the Canopy + Intensity model outperformed all other predictor sets tested (Fig. 3). The pseudo R^2 was 0.59 with an observed versus predicted R^2 of 0.64, a RMSD of $139.4\,g\,m^{-2}$, and a bias of $-9.7\,g\,m^{-2}$. The Canopy + Intensity model minimized the RMSD errors compared to the Canopy only model by $34.8\,g\,m^{-2}$ and by more than $80.0\,g\,m^{-2}$ when compared to the Topo or Intensity only models. The Topo and Intensity models performed very poorly, having RMSD errors over $220\,g\,m^{-2}$.

3.2.2. Lidar-derived biomass maps

The biomass maps produced using the Canopy + Intensity model visually correspond with landscape features and vegetation patterns across the study area, with shallow soil areas having low predicted biomass, and deeper soils and riparian areas having higher predicted

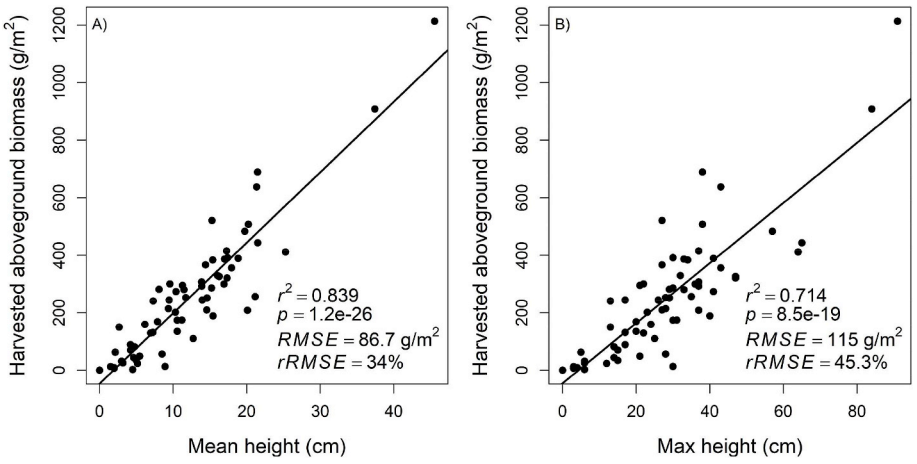

Fig. 2. Relationships between harvest aboveground biomass and mean vegetation height (a) and harvested aboveground vegetation biomass and max field height (b) across the 65 1-m vegetation plots. The linear model coefficient of determination (r^2), p-value (p), root mean square error (RMSE) and relative root mean square error (rRMSE) are shown for each relationship.

biomass (Fig. 4). Areas of low biomass had higher levels of model uncertainty, with higher biomass areas having much better model agreement, as displayed with the coefficient of variation map (Fig. 4B). For each pasture area (N = 23), the average estimated biomass was 172.97 g m^{-2} and ranged from 117.40 g m^{-2} to 233.27 g m^{-2}. The average 10th and 90th percentiles across all pasture areas varied with increasing pixel size, with the finest resolution (1.0668 m) data having the largest range between these two percentiles, and the coarsest resolution (30 m) having the smallest range (Table 4).

3.3. The impact of decreasing spatial resolution on measures of spatial heterogeneity

The boxplots created for each of the semivariogram-derived metrics show observably different measures across the six pixel sizes analyzed (Fig. 5). Only the range and the sill met the assumption of homogeneity of variance needed for Mann-Whitney U rank-sum tests. Using the Mann-Whitney *U* test to compare the distributions of the range statistic between each pixel size revealed that the 1.0668 m data was different from all other pixel sizes. Significant differences in the range metric were found across all other paired comparisons except between the 3 m and 5 m, the 5 m and 8 m, and the 20 m and 30 m pixel sizes (Fig. 5, Table S3). The 1.0668 m sill metric was also statistically different from all other pixel sizes. The sill metric at 3 m, 5 m and 8 m pixel size were similar (i.e., no significant difference between these pixel sizes) as were the 8 m, 20 m, and 30 m pixel sizes (Fig. 5, Table S4).

3.4. Identifying remotely sensed derived measures of spatial heterogeneity and summary statistics most sensitive to grazing intensity, and how this sensitivity changes with increasing spatial resolution of remotely sensed data

The summary statistics were more sensitive to grazing than the semivariogram statistics (Table 5 and Table S2) using Spearman rank correlations, linear and quadratic models. The only semivariogram statistic sensitive to grazing was the range statistic, and this significant relationship was exclusively observed across the 1.0668 m to 8 m pixel resolutions, using spearman rank, linear and quadratic models (Table 5, Table S2) with the 3 m resolution data having the highest r^2 value. The 75th percentile of biomass was significantly related to grazing intensity across all resolutions except the 1.0668 (Table 5) when all pastures were included (N = 23), and significant across all resolutions when we dropped the pasture with the greatest stocking rate (P5) due to its heavy influence on the summary statistic linear models (N = 22) (Fig. S7 (C and D) and Table S6). The pasture mean biomass statistic was found to be significantly correlated to stocking rates using the quadratic model and when using a linear model if the P5 pasture was dropped. The coefficient of variation was unique in that the only significant relationships were found with the quadratic models, and none with the linear models (See Supplemental Fig. S4-S12 for scatterplots).

4. Discussion

4.1. Modelling and mapping bunchgrass biomass with airborne lidar

The variables most useful to accurately quantify grassland biomass in all the predictor datasets were canopy volume, max height and mean intensity. Similar to Greaves et al. (2016), the inclusion of the canopy volume variable was important in the final Random Forest model.

Table 3
Variable selection for Random Forest models. The numbers indicate how many times each variable was selected across 1000 Random Forest model runs using the model selection tool in the 'rfUtilities' package. Dashes represent variables not included in the model selection when testing each predictor set. The final Random Forest model for each predictor set only included predictors selected across more than 500 of the model runs. The bolded predictor sets are plotted in Fig. 3.

Variable	Canopy	Topo	Intensity	Canopy + Topo	Canopy + Intensity	Intensity + Topo	Canopy + Topo + Intensity
Vol	**1000**	–	–	1000	**1000**	–	1000
Tot_Returns	0	–	–	0	0	–	0
H_Max	**1000**	–	–	1000	**912**	–	1000
Canopy_Dns	**969**	–	–	998	**0**	–	0
SWI	–	92	–	0	–	0	0
Aspect	–	0	–	0	–	0	0
Slope	–	**1000**	–	284	–	100	0
Curve	–	0	–	0	–	0	0
Int_Mean	–	–	**1000**	–	**1000**	1000	1000

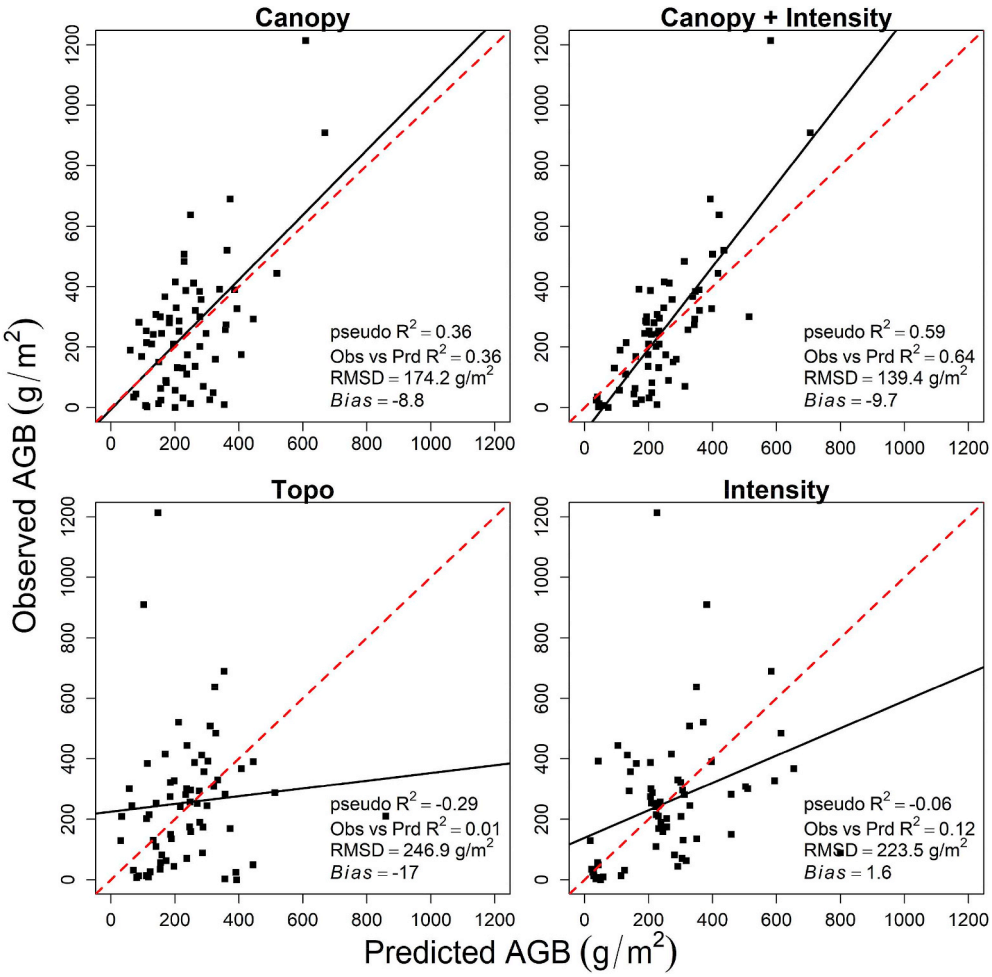

Fig. 3. Random Forest model results across the four datasets that produced a unique set of predictor variables. See Table 3 for predictors used. The black lines represent the best fit line, while the dotted red line represents the one-to-one line. (For interpretation of the references to color in this figure legend, the reader is referred to the Web version of this article.)

Volumetric measures have also proved useful for estimating vegetation biomass using ground-based lidar in an agricultural setting (Eitel et al., 2014), to assess fuel-bed characteristics (Loudermilk et al., 2009) and to quantify shrub biomass (Greaves et al., 2015). The return intensity variable also was important in the Random Forest model, likely due to the increased return intensity of the Leica ALS70 near-infrared laser (i.e. the 1064 nm wavelength) when contacting green vegetation as compared to bare ground or rock (Eitel et al., 2016a). Intensity data is increasingly being applied to quantify vegetation biochemistry (Eitel et al., 2016b, 2014) and separate wood from foliage to improve leaf area estimates of trees (Béland et al., 2014, 2011). In this study, the intensity metric was selected 100% of the time when it was included in any of the predictor datasets. The max height metric was the other lidar derived metric selected across all model runs when available as a predictor variable. It improved Random Forest model results (RMSD = 139.4 g m^{-2}) when compared to a model excluding it (RMSD = 148.56 g m^{-2}). In other studies, lidar-derived max height has been used to assess vegetation height and biomass in short-statured vegetation communities even though it typically underestimates the field measures (Kulawardhana et al., 2014). In this grassland system, due to the close relationship between the field measures of both the mean and max vegetation height with biomass (Fig. 2), it is logical that a max height lidar measure would be useful for modeling biomass. None of the topographic variables were selected more than 50% of the time when these variables were included with other variable datasets (Canopy or Intensity). We speculate that this could be due to the high degree of fine-scale topographic heterogeneity across this system and that the scale at which we computed topographic measures (1 m) does not align well with the processes linked to variations in biomass.

Our most accurate Random Forest model (Canopy + Intensity) had a pseudo R-squared of 0.59 and a RMSD of 139.4 g m^{-2}. This is a slightly better fit than was achieved in Wang et al. (2017) (R^2 = 0.34), who estimated grassland biomass generated from discrete lidar collected via an UAV, and Kulawardhana et al. (2014) (R^2 = 0.33 for total biomass) who used multiple linear regression to estimate salt marsh biomass based on discrete return lidar collected by airplane along with spectral data from NAIP imagery. The estimated biomass across the pasture areas with a mean of 174.74 g m^{-2} and a range of 117 g m^{-2} to 233.27 g m^{-2} are comparable to results from previous remote sensing studies in the Zumwalt Prairie that used Landsat data to assess biomass (Jansen et al., 2018, 2016). The power of these lidar-derived maps is their ability to capture fine-scale heterogeneity, enabling the visualization and quantification of fine-scale topographic- and management-related patterns of vegetation compared with coarse scale data provided by Landsat (Fig. 6). Results from this study demonstrate that in short-statured vegetation communities, the canopy volume and Random Forest modeling approach outlined by Greaves et al. (2016) can be applied to other short-statured vegetation communities such as grassland systems.

The non-uniform overlapping flight lines of the lidar acquisition caused variability in the point densities, which impacted the canopy metrics and subsequently the original biomass maps. We attribute the

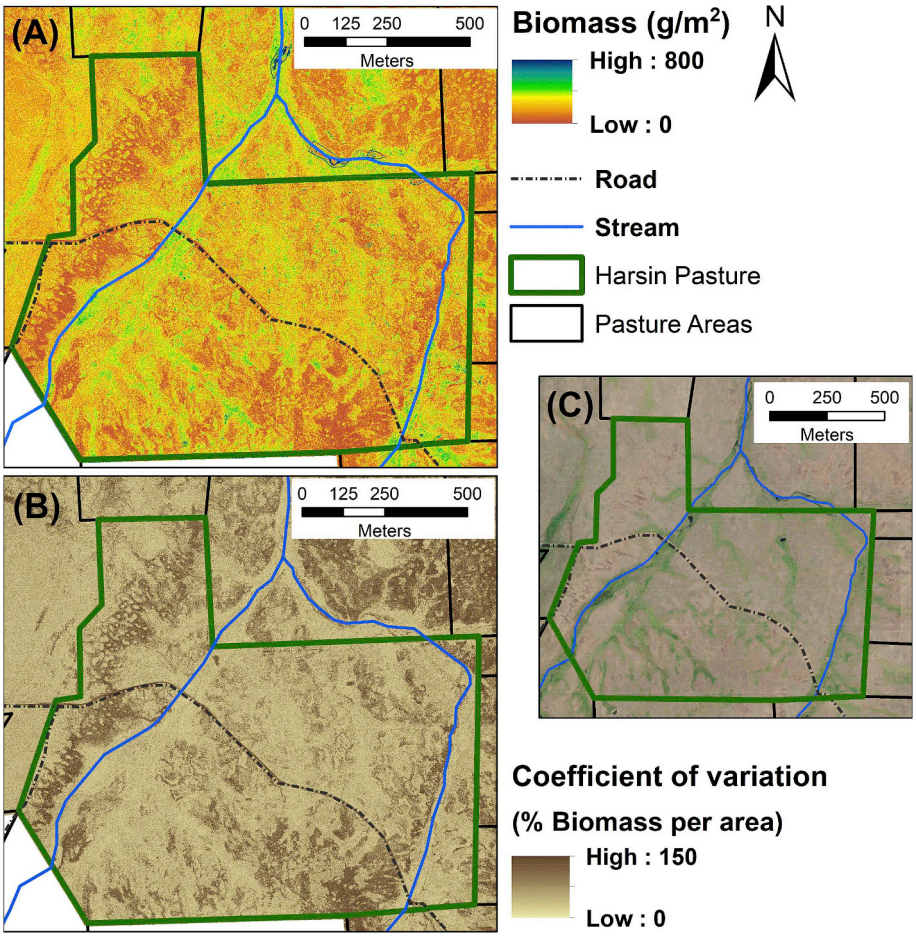

Fig. 4. Lidar-derived biomass map of the Harsin Pasture predicted from the best RF model at 1.0668 m resolution (A) along with a map of the coefficient of variation of estimated aboveground biomass (B) and the 2014 NAIP imagery displayed in true color (RGB) (C).

Table 4
Pasture-level modeled biomass summary statistics (N = 23) across the varying pixel sizes.

Pixel Size	Mean	Min	Max	10th percentile	90th percentile	CV
1.0668	173.70	117.20	233.08	66.82	288.54	0.51
3	173.75	117.18	233.21	95.62	254.23	0.37
5	173.82	117.23	233.24	100.54	247.96	0.34
8	173.94	117.38	233.46	104.50	243.20	0.32
20	174.22	117.76	233.75	112.63	234.87	0.28
30	174.21	117.67	234.01	115.71	231.50	0.27

striping effects to the variability in the overlapping flight lines and end of scans rather than the intensity data, because the intensity data was post processed and exhibited no striping effects (Fig. S1:E). For future studies, lidar acquisition specifically for grassland assessment could be improved by acquiring a more uniform point cloud across the study area, with a point density of greater than 9 points m^{-2}. This would potentially eliminate the need to normalize the point cloud density to reduce striping effects observed in the biomass (Fig. S1:A-D). Furthermore, this would likely increase modeling accuracies. Our first analysis attempt with non-corrected point clouds had better accuracy (Fig. S2) compared to the final models presented here, due to a higher average point density across the sample biomass quadrats. However, the lower point density in select places within the study area precluded extrapolation of these early models across the entire study area.

4.2. The impact of spatial resolution on measures of spatial heterogeneity

The aggregation of the fine-scale data to coarser scales revealed patterns similar to those described by Jupp et al. (1988); Wiens (1989); Woodcock et al. (1988); Woodcock and Strahler (1987), in that the overall variance (i.e., the sill) and fine scale variation (i.e., nugget) of the data were reduced, and the range increased (Fig. 7). In testing the differences in the semivariogram measures across all pixel sizes, the impact of aggregation is significant. This indicates that the semivariogram statistics provide different measures as the pixel size changes. In selecting a plot size or spatial resolution to study a process and phenomena it is important to know how that decision impacts your findings (Wiens, 1989); here we see that biomass data quantified at the 1.0668 m pixel resolution provides statistically different spatial measures compared to the spatial measures when aggregated to larger pixel sizes.

Following ideas in Strahler et al. (1986) on the discrete scene model, when quantifying grassland vegetation with remotely sensed data, the resolution would be considered low (i.e. coarse) when compared to a single leaf or single plant that is smaller than the size of the pixel but can be considered high (i.e., fine) if related to vegetation patches or pasture areas that are larger than the pixel being used for analysis. Using this rationale, our finest-resolution data (i.e., 1.0668 m) is not high-resolution data at the individual plant level due to pixels containing numerous other spectra (Asner, 2004) such as soil, rock or plant

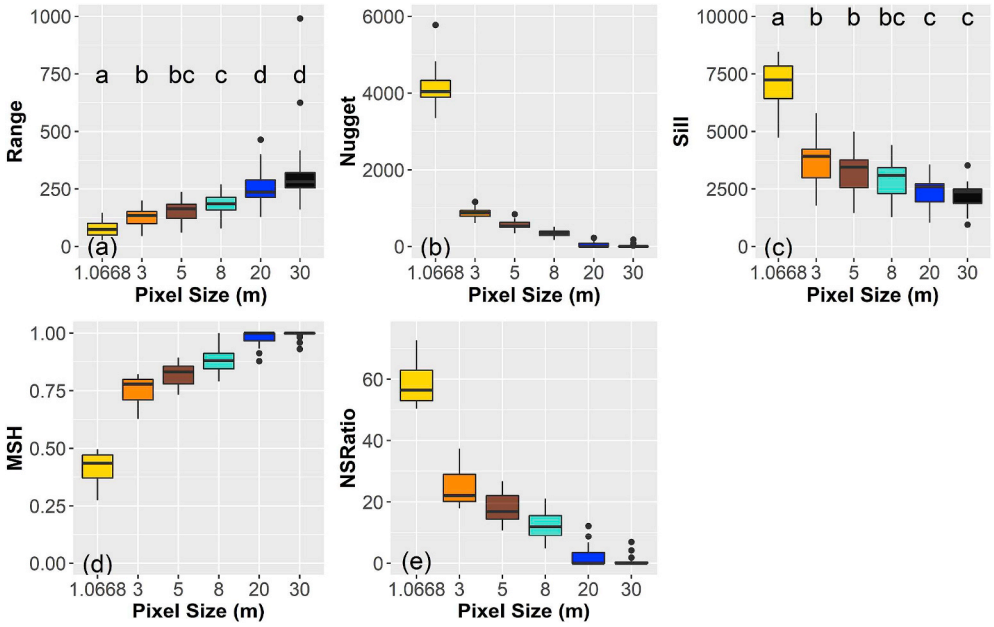

Fig. 5. Boxplots of semivariogram metrics from each of the 23 study pastures by pixel size (N = 23). The bold black lines in the middle of each colored box represent the median value (50th percentile), with the lower and upper limits of the box representing the 25th and 75th percentile respectively. The whiskers extend to the smallest and largest values falling within 1.5 times the associated value (lower value = 25th percentile, upper value = 75th percentile) of the interquartile range. The black dots represent outliers. Significant differences found between the pixel sizes using the Mann-Whitney/Wilcoxon test for each semivariogram statistic that met the assumption of homogeneity of variance (Range and Sill) are indicated with different letters. Statistic Abbreviations are as follows: MSH = magnitude of spatial heterogeneity and NSRatio = nugget to sill ratio.

Table 5
Regression model results between pasture level summary and spatial statistics and stocking rate (N = 23). The coefficients of determination values (r^2) that are significant at $\alpha = 0.05$ are shown in bold with boxes around them. The italicized underlined values are models that violated assumptions of linear models. Statistic Abbreviations are as follows: Per10 = 10th Percentile, Per25 = 25th Percentile, Per75 = 75 Percentile, Per90 = 90th Percentile, CV = Coefficient of Variation, MSH = Magnitude of Spatial Heterogeneity, NSR = Nugget to Sill Ratio. The transformation abbreviations are as follows: Recip = OLS using a reciprocal transformation on the predictor variable, None-OLR = one outlier was removed with no transformation performed on the data; Quad = Quadratic model was used.

		Pixel Size					
Statistic	**Transform**	**1.0668m**	**3m**	**5m**	**8m**	**20m**	**30m**
Per10	Recip	0.04	0.05	0.05	0.06	0.07	0.08
Per10	Quad	0.23	0.23	0.24	0.24	**0.27**	**0.29**
Per10	None-OLR	0.12	0.14	0.14	*0.14*	0.17	0.18
Per25	None	0.08	0.07	0.07	0.08	0.09	0.09
Per25	Quad	**0.27**	**0.28**	**0.28**	**0.28**	**0.28**	**0.28**
Per25	None-OLR	**0.18**	0.17	0.17	0.17	**0.19**	**0.19**
Mean	None	0.13	0.13	0.13	0.13	0.13	0.13
Mean	Quad	**0.30**	**0.29**	**0.30**	**0.30**	**0.30**	**0.29**
Mean	None-OLR	**0.29**	**0.29**	**0.29**	**0.29**	**0.30**	**0.29**
Per75	None	0.15	**0.17**	**0.18**	**0.18**	**0.18**	**0.18**
Per75	Quad	**0.26**	**0.29**	**0.29**	**0.29**	**0.30**	**0.29**
Per75	None-OLR	**0.23**	**0.26**	**0.26**	**0.27**	**0.27**	**0.26**
Per90	None	*0.17*	*0.20*	*0.20*	*0.19*	*0.18*	*0.17*
Per90	Quad	0.23	**0.27**	*0.27*	**0.27**	**0.27**	0.25
Per90	None-OLR	*0.23*	**0.28**	**0.28**	**0.28**	*0.27*	*0.26*
CV	None	0.05	0.03	0.03	0.03	0.05	0.05
CV	Quad	**0.28**	**0.26**	0.26	**0.26**	**0.27**	**0.29**
CV	None - OLR	0.13	0.10	0.09	0.10	0.12	0.12
Range	none	**0.23**	**0.40**	**0.37**	**0.25**	0.01	*0.02*
Range	Quadratic	**0.42**	**0.54**	**0.45**	**0.28**	*0.02*	*0.07*
Range	Recip - OLR	**0.19**	**0.29**	**0.27**	**0.26**	0.139	0.099
Sill	None	0.03	0.01	*0.01*	0.00	0.00	0.01
Sill	Quad	0.07	0.10	0.10	0.10	0.09	0.07
Nugget	None	0.02	0.00	0.00	0.00	*0.03*	*0.09*
Nugget	Quad	0.02	0.09	0.09	0.02	0.14	0.12
MSH	None	*0.02*	*0.03*	0.01	*0.00*	*0.03*	*0.09*
MSH	Quad	*0.12*	*0.07*	*0.03*	*0.07*	*0.15*	*0.12*
NSR	None	0.02	0.03	0.01	0.00	0.03	0.09
NSR	Quad	0.12	0.07	0.03	0.05	0.15	0.12

species at a different phenological stage. This is evident from the large average nugget and when plotting semivariograms for each resolution for a single pasture (Fig. 7). The nugget can represent noise, sampling error, or the within pixel variation. In this study, we reason that the large nugget with the 1.0668 m data is largely driven by within pixel variation between bunchgrass vegetation and soil. When we aggregate these data to coarser scales (3 m to 30 m), we smooth over the canopy gaps and reduce the variability in biomass, thus decreasing the nugget (semivariance) captured at fine scales.

Specifically exploring the range data at the finest resolution (~1.0668 m), we obtained an average range of 78.8 m across all study pastures. This range aligns with a previous study conducted in a mixed grassland in Saskatchewan, Canada which used a handheld spectroradiometer and found a range of 70 m using a leaf area index metric (He et al., 2006). From previous remote sensing grassland studies which determined the optimum pixel size to quantify grassland ecosystems, both Rahman et al. (2003) and He et al. (2006), point to sampling theories which state that in order to effectively measure objects, one must use a pixel size equal to or less than one half the size of the object (i.e. the range) of interest. Following this rationale, to effectively quantify aboveground biomass across these pasture areas, a pixel size less than 40 m would be suitable given our average range of 78.8 m. Interestingly, when using the coarsest resolution (20 m to 30 m) from this analysis to quantify how spatial patterns of biomass correlate to grazing, these data failed to produce significant relationships (See 4.3 below).

4.3. Identifying the measures of spatial heterogeneity most sensitive to grazing intensity and how this sensitivity changes with increasing spatial resolution of remotely sensed data

It is well documented that grazing can impact various aspects of vegetation heterogeneity such as species composition, structure and biomass (Adler et al., 2001; Fuhlendorf and Engle, David, 2001), yet the ability to quantify and monitor spatial heterogeneity of vegetation amount (i.e., biomass, cover, height) with remotely sensed data is dependent on the interaction between the spatial resolution of the data and the vegetation pattern on the ground. It is known that some resolutions will be too coarse to detect vegetation patterns (Wiens, 1989). In this study, testing the relationship between grazing intensity and the

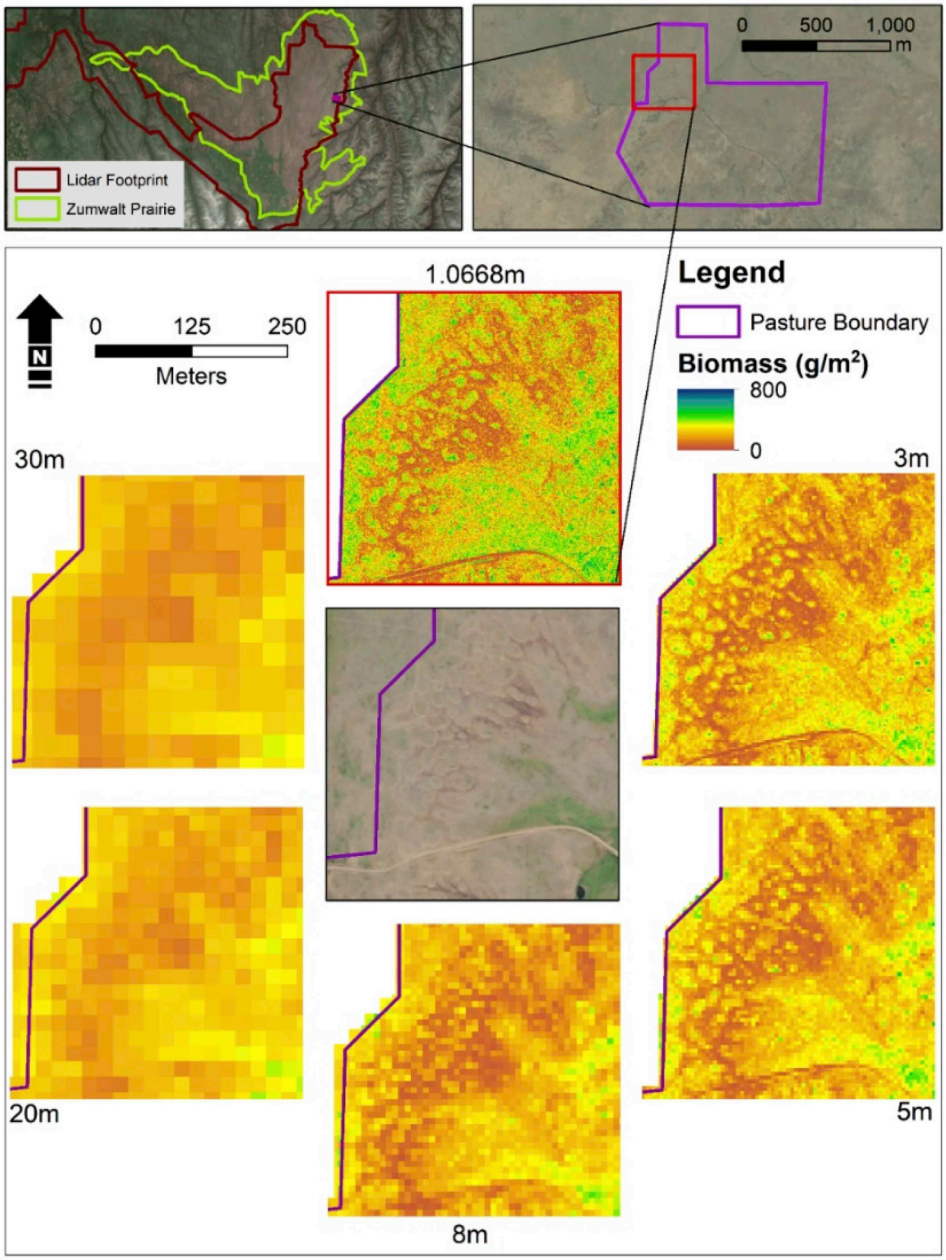

Fig. 6. Grassland biomass at varying pixel sizes (1.0668 m, 3 m, 5 m, 8 m, 20 m, and 30 m), produced by aggregating 1.0688 m lidar derived biomass data for the Zumwalt Prairie in northeast Oregon.

semivariogram-derived measures of heterogeneity across the various pixel sizes revealed that the range statistic was the only spatial statistic sensitive to grazing. We also observed that the sensitivity of this range statistic to grazing became weaker as the pixel size increased, so that the 20 m and 30 m resolutions failed to provide significant relationships with grazing intensity. Ecologically, this may reflect the decrease in variance that accompanies aggregation to coarser resolutions. Both grazing and coarsening of the pixel size resolution has a dampening effect on the variability of estimated biomass per pixel across the pasture areas in this study area, likely related to the typical size of the large quantity vegetation patches and the bare ground areas being small, less than 8 m in size.

The results showing an increase in the variogram-derived range metric with higher grazing intensity are similar to Scarth and Trevithick (2017), who observed increases in the range value with increased grazing using 10 m Sentinel-2 bare ground data in Australia. That the range value increased with grazing intensity contradicts Virk and Mitchell (2015), who after two years found that grazing decreased the semivariogram range statistics. Virk and Mitchell (2015) also found that the MSH was sensitive to grazing and increased with grazing over the course of their study, whereas our results showed that this metric was not sensitive to grazing intensity at any scale. These differences are likely due to underlying differences in vegetation heterogeneity, grazing distribution and intensity (Adler et al., 2001), and the study length. Virk and Mitchell (2015) tracked vegetation across multiple years to monitor the change in heterogeneity with varying levels of grazing. Here we only use one year of data, which is not ideal, especially in grassland systems that can experience large year-to-year variations in production (Briske et al., 2015). Another influence could be that Virk and Mitchell (2015) modeled live biomass using NDVI, which can be impacted by standing dead vegetation and litter in natural grassland systems (Jansen et al., 2018; Xu et al., 2014). Mapping the pattern of green vegetation only could potentially increase measures of heterogeneity.

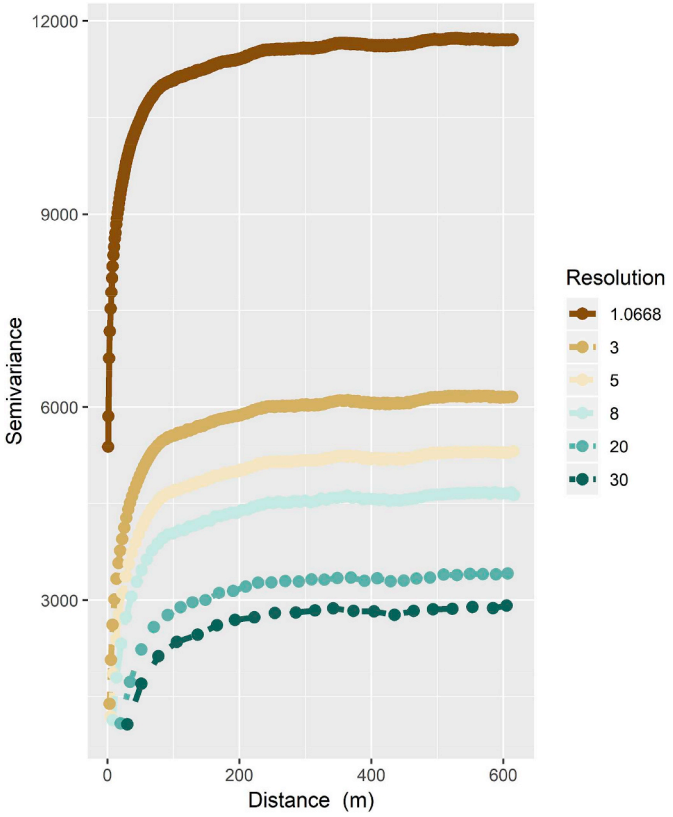

Fig. 7. Empirical semivariograms for the Harsin pasture using the six different increasing pixel resolutions.

Following Adler et al., 2001 there are two ways grazing decreases heterogeneity:1) when grazing is guided by the vegetation pattern and selective grazing decreases contrast between vegetation types or 2) with patch or homogeneous grazing, when the grazing pattern is weaker than the vegetation pattern (Adler et al., 2001). From this study, we reason that selective grazing across the study area decreases the contrast in vegetation biomass, leading to reduced heterogeneity with greater stocking rates. That the range statistic was not significantly related to grazing at the 20 m and 30 m scale shows how the spatial scale used to study a pattern or process may influence the interpretation of results, and that these processes can be expressed differently depending on the scale at which they are studied (Townsend and Fuhlendorf, 2010). In other words, while the 30 m scale may be suitable to monitor vegetation biomass and a general change in quantity, this scale is not sensitive enough to detect changes in the spatial vegetation pattern (i.e. spatial heterogeneity measured with a spatial statistic) induced by grazing in this grassland.

4.4. Implications for management and future analysis opportunities

The maps created using the Random Forest model provide the first landscape-scale maps of grassland biomass derived from airplane-gathered lidar in this grassland system and, to our knowledge, in any short-stature vegetation grassland. Fine-scale vegetation datasets such as this one can provide spatially explicit information on vegetation structure and biomass which can then be related to habitat requirements for critical species (Boelman et al., 2016; Vierling et al., 2008). They also provide data to better understand how management drivers impact vegetation biomass and structure at fine scales. For example, in this grassland system, grazing was associated with an increasing range metric, suggesting a reduction in fine-scale biomass heterogeneity. This result can inform conservation and management actions which seek to increase habitat heterogeneity. Linking semivariogram-derived range metrics to other biological processes, such as erosion or weed invasion, as well as habitat requirements for wildlife species such as birds, would further reveal how this dataset and resulting spatial metrics could be used to monitor meaningful conservation indicators.

The result that the 20 m and 30 m data, analogous to the spatial resolution of Sentinel-2 and Landsat respectively, did not produce spatial heterogeneity metrics sensitive to grazing provides evidence that these sensors are not best suited to monitor how grazing impacts aboveground biomass heterogeneity vegetation in this study area. Finer resolution data are available for purchase (e.g., WorldView-3, Planet Labs, Inc., RapidEye) which could be used to monitor the effect of grazing on spatial heterogeneity over time, but in this grassland, prior research has indicated that a shortwave infrared band is necessary to achieve maximum accuracy due to a large component of the aboveground biomass being standing dead or senescent vegetation (Jansen et al., 2018, 2016). While the spatial heterogeneity metrics were not sensitive to grazing at coarser resolutions (i.e., 20 m, 30 m), the coefficient of variation (CV) metric was. This metric is often used as a non-spatial measure of heterogeneity (Adler et al., 2001) and was significantly related to grazing across all scales using a quadratic model. This finding is supported by Johnson et al. (2011), who modeled a significant quadratic effect of grazing on the structural heterogeneity across this same study area. In both studies, it was observed that coefficient of variation increased as grazing increased from no grazing to moderate grazing and decreased from moderate grazing to heavy grazing. This finding suggests that Landsat data at the 30 m scale can provide reliable estimates of this non-spatial heterogeneity measure.

Future studies investigating how grazing management impacts vegetation heterogeneity should explore additional spatial statistics at larger spatial extents and temporal scales. For example, spatial statistics such as Moran's I could be computed at the pasture and ranch scale over time, which would contribute to an improved understanding of the hierarchal and nested nature of this ecosystem, and how land management impacts heterogeneity at scales relevant to landscape processes and management (Fuhlendorf et al., 2012). It could also be informative to analyze the fine scale biomass data with an object-based approach for mapping vegetation patches as well as for habitat classification. Ideally, this approach segments spatial data based on meaningful ecological patterns, helping to overcome issues of information loss due to arbitrarily defined pixel areas (Karl and Maurer, 2010). Studying processes that interact with grazing to impact vegetation patterns, such as fire and soil characteristics, is another future area of interest.

4.5. Conclusion

Lidar data collected by airplane across landscape scales can provide significant relationships with short-statured grassland biomass for fine grain mapping (~1 m resolutions) of vegetation pattern at landscape- and pasture-level scales. Coupling mapped biomass data with grazing data helps to provide a relevant management-scale understanding of how grazing impacts biomass heterogeneity or patterns across pastures. Aggregating the fine-scale biomass data to increasingly coarser pixel sizes reveals how the spatial resolution of data impacts our ability to quantify spatial patterns of processes under question. This information in turn informs the selection of the most appropriate sensor/spatial resolution to quantify or monitor a desired phenomenon or ecological process. For example, when using semivariograms to study spatial heterogeneity, we found that high-resolution datasets with pixel sizes between 1 m and 8 m are needed to monitor the effect of grazing on vegetation pattern at peak biomass across this short-statured, highly heterogeneous grassland. Ecologically, we found evidence that grazing decreases the spatial heterogeneity of aboveground biomass within this grassland system, and we identified the spatial resolution (1 m to 8 m) at which the process is most evident using gridded data. This is an important finding for future research and monitoring as well as current

management practices which seek to increase heterogeneity in this and other similar grassland ecosystems.

Acknowledgements

Funding was provided by The Nature Conservacy's Oren Pollak Student Research Grant, the Priscilla Bullitt Collins Trust Northwest Conservation Fund and The Nature Conservancy. We thank Jeff Fields and Derek Johnson, and the Oregon Chapter of TNC for the continued support and funding of the lidar acquisition over the Zumwalt Prairie. We also thank Lee Vierling for sharing his GPS equipment and knowledge of field and analysis methods. We are also grateful to Eva Strand, Robert V. Taylor and Heidi Schmalz for methodological and editorial feedback during the creation of this manuscript. We also thank Brent Wydrinski for lending a hand in the field. We also thank the three anonymous reviewers who provided valuable feedback which greatly improved this manuscript.

Appendix A. Supplementary data

Supplementary data to this article can be found online at https://doi.org/10.1016/j.rse.2019.111432.

References

Adler, P., Raff, D., Lauenroth, W., 2001. The effect of grazing on the spatial heterogeneity of vegetation. Oecologia 128, 465–479. https://doi.org/10.1007/s004420100737.

Adler, P.B., Milchunas, D.G., Lauenroth, W.K., Sala, O.E., Burke, I.C., 2004. Functional traits of graminoids in semi-arid steppes: a test of grazing histories. J. Appl. Ecol. 41, 653–663. https://doi.org/10.1111/j.0021-8901.2004.00934.x.

Allen-Diaz, B., Chapin, F.S., Diaz, S., Howden, M., J.P., Smith, M.S., 1995. Rangelands in a changing climate: impacts, adaptations, and mitigation. In: Watson, W.T., Zinyowera, M.C., Moss, R.H., Dokken, D.J. (Eds.), Clim. Chang. 1995—Impacts, Adapt. Mitigation, pp. 131–158.

Anderson, G.L., Hanson, J.D., Hass, R.H., 1993. Evaluating Landsat thematic mapper derived vegetation indices for estimating above-ground biomass on semiarid rangelands. Remote Sens. Environ. 45, 165–175.

Asner, G.P., 2004. Biophysical remote sensing signatures of arid and semiarid ecosystems. In: Remote Sensing for Natural Resources Management and Environmental Monitoring: Manual of Remote Sensing, vol. 4. pp. 53–110.

Augustine, D.J., McNaughton, S.J., 1998. Ungulate effects on the functional species composition of plant communities: herbivore selectivity and plant tolerance. Source J. Wildl. Manag. 62, 1165–1183. https://doi.org/10.2307/3801981.

Béland, M., Baldocchi, D.D., Widlowski, J.L., Fournier, R.A., Verstraete, M.M., 2014. On seeing the wood from the leaves and the role of voxel size in determining leaf area distribution of forests with terrestrial LiDAR. Agric. For. Meteorol. 184, 82–97. https://doi.org/10.1016/j.agrformet.2013.09.005.

Béland, M., Widlowski, J.L., Fournier, R.A., Côté, J.F., Verstraete, M.M., 2011. Estimating leaf area distribution in savanna trees from terrestrial LiDAR measurements. Agric. For. Meteorol. 151, 1252–1266. https://doi.org/10.1016/j.agrformet.2011.05.004.

Benkobi, L., Uresk, D.W., Schenbeck, G., King, R.M., 2000. Protocol for monitoring standing crop in grasslands using visual obstruction. J. Range Manag. 53, 627–633.

Bestelmeyer, B.T., Briske, D.D., 2012. Grand challenges for resilience-based management of rangelands. Rangel. Ecol. Manag. 65, 654–663. https://doi.org/10.2111/REM-D-12-00072.1.

Boehner, J., Koethe, R., Conrad, O., Gross, J., Ringeler, A., Selige, T., 2002. Soil regionalisation by means of terrain analysis and process parameterisation. In: Status Prospect Soil Inf. South - East. Eur. Soil Databases, Proj. Appl., vols. 1–4978-92-79-04972-9, .

Boelman, N.T., Holbrook, J.D., Greaves, H.E., Krause, J.S., Chmura, H.E., Magney, T.S., Perez, J.H., Eitel, J.U.H., Gough, L., Vierling, K.T., Wing, J.C., Vierling, L.A., 2016. Airborne laser scanning and spectral remote sensing give a bird ' s eye perspective on arctic tundra breeding habitat at multiple spatial scales. Remote Sens. Environ. 184, 337–349.

Booth, D.T., Tueller, P.T., 2003. Rangeland monitoring using remote sensing. Arid Land Res. Manag. 17, 455–467.

Breiman, L., 2001. Random forests. Mach. Learn. 45, 5–32.

Briske, D.D., Joyce, L. a, Polley, H.W., Brown, J.R., Wolter, K., Morgan, J. a, McCarl, B. a, Bailey, D.W., 2015. Climate-change adaptation on rangelands: linking regional exposure with diverse adaptive capacity. Front. Ecol. Environ. 13, 249–256. https://doi.org/10.1890/140266.

Cambardella, C.A., Moorman, T.B., Parkin, T.B., Karlen, D.L., Novak, J.M., Turco, R.F., Konopka, A.E., 1994. Field-scale variability of soil properties in central Iowa soils. Soil Sci. Soc. Am. J. 58, 1501. https://doi.org/10.2136/sssaj1994.03615995005800050033x.

Cooper, S.D., Roy, D.P., Schaaf, C.B., Paynter, I., 2017. Examination of the potential of terrestrial laser scanning and structure-from-motion photogrammetry for rapid nondestructive field measurement of grass biomass. Remote Sens. 9. https://doi.org/10.3390/rs9060531.

Crookston, N., Finley, A., 2008. yaImpute: an R Package for kNN Imputation. J. Stat. Softw. 23.

Eitel, J.U.H., Höfle, B., Vierling, L.A., Abellán, A., Asner, G.P., Deems, J.S., Glennie, C.L., Joerg, P.C., LeWinter, A.L., Magney, T.S., Mandlburger, G., Morton, D.C., Müller, J., Vierling, K.T., 2016a. Beyond 3-D: the new spectrum of lidar applications for earth and ecological sciences. Remote Sens. Environ. 186, 372–392. https://doi.org/10.1016/j.rse.2016.08.018.

Eitel, J.U.H., Magney, T.S., Vierling, L.A., Brown, T.T., Huggins, D.R., 2014. Field Crops Research LiDAR based biomass and crop nitrogen estimates for rapid , non-destructive assessment of wheat nitrogen status. Field Crop. Res. 159, 21–32. https://doi.org/10.1016/j.fcr.2014.01.008.

Eitel, J.U.H., Magney, T.S., Vierling, L.A., Greaves, H.E., Zheng, G., 2016b. An automated method to quantify crop height and calibrate satellite-derived biomass using hypertemporal lidar. Remote Sens. Environ. 187, 414–422. https://doi.org/10.1016/j.rse.2016.10.044.

Fleischner, T.L., 1994. Ecological costs of livestock grazing in western north America. Conserv. Biol. 8, 629–644. https://doi.org/10.1046/j.1523-1739.1994.08030629.x.

Forsmoo, J., Anderson, K., Macleod, C.J.A., Wilkinson, M.E., Brazier, R., 2018. Drone-based structure-from-motion photogrammetry captures grassland sward height variability. J. Appl. Ecol. 55, 2587–2599. https://doi.org/10.1111/1365-2664.13148.

Fortin, M.-J., Dale, M., 2005. Spatial Analysis: A Guide for Ecologists. Cambridge University Press, Cambridge.

Friedel, M.H., Chewings, V.H., Bastin, G.N., 1988. The use of comparative yield and dry-weight-rank tech- niques for monitoring arid rangeland. J. Range Manag. 41, 430–435.

Friedl, M., Michaelsen, J., Davis, F., Walker, H., Schimel, D., 1994. Estimating grassland biomass and leaf area index using ground and satellite data. Int. J. Remote Sens. 15, 1401–1420.

Fu, B.J., Liu, S.L., Ma, K.M., Zhu, Y.G., 2004. Relationships between soil characteristics, topography and plant diversity in a heterogeneous deciduous broad-leaved forest near Beijing , China. Plant Soil 47–54.

Fuhlendorf, S.D., Engle, David, M., 2001. Restoring heterogeneity on Rangelands : ecosystem management based on evolutionary grazing patterns. Bioscience 51, 625–632.

Fuhlendorf, S.D., Engle, D.M., Elmore, R.D., Limb, R.F., Bidwell, T.G., 2012. Conservation of pattern and process: developing an alternative paradigm of rangeland management. Rangel. Ecol. Manag. 65, 579–589. https://doi.org/10.2111/REM-D-11-00109.1.

Gessler, P.E., Chadwick, O.A., Chamran, F., Althouse, L., Holmes, K., 2000. Modeling soil – landscape and ecosystem properties using terrain attributes. Soil Sci. Soc. Am. J. 64, 2046–2056.

Getis, A., Ord, J.K., 1992. The Analysis of Spatial Association, vol. 24.

Gholizadeh, H., Gamon, J.A., Townsend, P.A., Zygielbaum, A.I., Helzer, C.J., Hmimina, G.Y., Yu, R., Moore, R.M., Schweiger, A.K., Cavender-Bares, J., 2019. Detecting prairie biodiversity with airborne remote sensing. Remote Sens. Environ. 221, 38–49. https://doi.org/10.1016/j.rse.2018.10.037.

Gillan, J.K., McClaran, M.P., Swetnam, T.L., Heilman, P., 2019. Estimating forage utilization with drone-based photogrammetric point clouds. Rangel. Ecol. Manag. 72, 575–585. https://doi.org/10.1016/j.rama.2019.02.009.

Glenn, N.F., Neuenschwander, A., Vierling, L.A., Spaete, L., Li, A., Shinneman, D.J., Pilliod, D.S., Arkle, R.S., Mcilroy, S.K., 2015. Remote Sensing of Environment Landsat 8 and ICESat-2 : performance and potential synergies for quantifying dryland ecosystem vegetation cover and biomass ☆. Remote Sens. Environ. https://doi.org/10.1016/j.rse.2016.02.039.

Godínez-Alvarez, H., Herrick, J.E., Mattocks, M., Toledo, D., Van Zee, J., 2009. Comparison of three vegetation monitoring methods: their relative utility for ecological assessment and monitoring. Ecol. Indicat. 9, 1001–1008. https://doi.org/10.1016/j.ecolind.2008.11.011.

Greaves, H.E., Vierling, L.a., Eitel, J.U.H., Boelman, N.T., Magney, T.S., Prager, C.M., Griffin, K.L., 2015. Estimating aboveground biomass and leaf area of low-stature Arctic shrubs with terrestrial LiDAR. Remote Sens. Environ. 164, 26–35. https://doi.org/10.1016/j.rse.2015.02.023.

Greaves, H.E., Vierling, L.A., Eitel, J.U.H., Boelman, N.T., Magney, T.S., Prager, C.M., Grif, K.L., 2016. High-resolution mapping of aboveground shrub biomass in Arctic tundra using airborne lidar and imagery. Remote Sens. Environ. 184, 361–373.

Guerschman, J.P., Scarth, P.F., Mcvicar, T.R., Renzullo, L.J., Malthus, T.J., Stewart, J.B., Rickards, J.E., Trevithick, R., 2015. Remote Sensing of Environment Assessing the effects of site heterogeneity and soil properties when unmixing photosynthetic vegetation , non-photosynthetic vegetation and bare soil fractions from Landsat and MODIS data. Remote Sens. Environ. 161, 12–26. https://doi.org/10.1016/j.rse.2015.01.021.

He, Y., Guo, X., Wilmshurst, J., Si, B.C., 2006. Studying mixed grassland ecosystems II: optimum pixel size. Can. J. Remote Sens. 32, 108–115. https://doi.org/10.5589/m06-018.

Heady, H.F., 1957. The measurement and value of plant height in the study of herbaceous vegetation. Ecology 38, 313. https://doi.org/10.2307/1931691.

Hempson, G.P., Archibald, S., Bond, W.J., Ellis, R.P., Grant, C., Kruger, F.J., Kruger, L.M., Moxley, C., Peel, M.J.S., Smit, I.P.J., Vickers, K.J., 2015. Ecology of grazing lawns in Africa. Biol. Rev. 90, 979–994. https://doi.org/10.1111/brv.12145.

Herrick, J.E., Lessard, V.C., Spaeth, K.E., Shaver, P.L., Dayton, R.S., Pyke, D.A., Jolley, L., Goebel, J.J., 2010. National ecosystem assessments supported by scientific and local knowledge. Front. Ecol. Environ. 8, 403–408. https://doi.org/10.1890/100017.

Hudak, A.T., Evans, J.S., Smith, A.M.S., 2009. LiDAR utility for natural resource managers. Remote Sens. 1, 934–951. https://doi.org/10.3390/rs1040934.

Hudak, A.T., Wessman, C.A., 1998. Textural analysis of historical aerial photography to

characterize woody. Plant Encroachment in South African Savanna 330, 317–330.
Jacques, D.C., Kergoat, L., Hiernaux, P., Mougin, E., Defourny, P., 2014. Monitoring dry vegetation masses in semi-arid areas with MODIS SWIR bands. Remote Sens. Environ. 153, 40–49. https://doi.org/10.1016/j.rse.2014.07.027.
Jansen, V., Kolden, C., Schmalz, H., 2018. The development of near real-time biomass and cover estimates for adaptive rangeland management using Landsat 7 and Landsat 8 surface reflectance products. Remote Sens. 10, 1057. https://doi.org/10.3390/rs10071057.
Jansen, V.S., Kolden, C.A., Taylor, R.V., Newingham, A.B., 2016. Quantifying livestock effects on bunchgrass vegetation with Landsat ETM+ data across a single growing season. Int. J. Remote Sens. 37, 150–175. https://doi.org/10.1080/01431161.2015.1117681.
Johansen, K., Coops, N.C., Gergel, S.E., Stange, Y., 2007. Application of high spatial resolution satellite imagery for riparian and forest ecosystem classification. Remote Sens. Environ. 110, 29–44. https://doi.org/10.1016/j.rse.2007.02.014.
Johnson, T.N., Kennedy, P.L., DelCurto, T., Taylor, R.V., 2011. Bird community responses to cattle stocking rates in a Pacific Northwest bunchgrass prairie. Agric. Ecosyst. Environ. 144, 338–346. https://doi.org/10.1016/j.agee.2011.10.003.
Jupp, D.L.B., Strahler, A.H., Woodcock, C.E., 1988. Autocorrelation and regularization in digital images I. Basic theory. IEEE Trans. Geosci. Remote Sens. 26, 463–473. https://doi.org/10.1109/36.3050.
Karl, J.W., Maurer, B.A., 2010. Multivariate correlations between imagery and field measurements across scales: comparing pixel aggregation and image segmentation. Landsc. Ecol. 25, 591–605. https://doi.org/10.1007/s10980-009-9439-4.
Kimoto, C., DeBano, S., Thorp, R., 2012. Investigating temporal patterns of a native bee community in a remnant North American bunchgrass prairie using blue vane traps. J. Insect Sci. 12, 1–23.
Kulawardhana, R.W., Popescu, S.C., Feagin, R.a., 2014. Fusion of lidar and multispectral data to quantify salt marsh carbon stocks. Remote Sens. Environ. 154, 345–357. https://doi.org/10.1016/j.rse.2013.10.036.
Lane, D.R., BassiriRad, H., 2005. Diminishing spatial heterogeneity in soil organic matter across a prairie restoration chronosequence. Restor. Ecol. 13, 403–412. https://doi.org/10.1111/j.1526-100X.2005.00050.x.
Lechner, A.M., Stein, A., Jones, S.D., Ferwerda, J.G., 2009. Remote sensing of small and linear features: quantifying the effects of patch size and length, grid position and detectability on land cover mapping. Remote Sens. Environ. 113, 2194–2204. https://doi.org/10.1016/j.rse.2009.06.002.
Li, A., Dhakal, S., Glenn, N.F., Spaete, L.P., Shinneman, D.J., Pilliod, D.S., Arkle, R.S., McIlroy, S.K., 2017. Lidar aboveground vegetation biomass estimates in shrublands: prediction, uncertainties and application to coarser scales. Remote Sens. 9. https://doi.org/10.3390/rs9090903.
Li, H., Reynolds, J.F., 1994. A simulation experiment to quantify spatial heterogeneity in categorical maps. Ecology 75, 2446–2455.
Liaw, A., Wiener, M., 2002. Classification and regression by randomForest. R. News 2, 18–22.
Lin, Y., Hong, M., Han, G., Zhao, M., Bai, Y., Chang, S.X., 2010. Grazing intensity affected spatial patterns of vegetation and soil fertility in a desert steppe. Agric. Ecosyst. Environ. 138, 282–292. https://doi.org/10.1016/j.agee.2010.05.013.
Loudermilk, E.L., Hiers, J.K., O'Brien, J.J., Mitchell, R.J., Singhania, A., Fernandez, J.C., Cropper, W.P., Slatton, K.C., 2009. Ground-based LIDAR: a novel approach to quantify fine-scale fuelbed characteristics. Int. J. Wildland Fire 18, 676–685. https://doi.org/10.1071/WF07138.
Mack, R.N., Pyke, D.A., 1983. The demography OF bromus tectorum: variation IN time and space. J. Ecol. 71, 69–93.
Marsett, R.C., Qi, J., Heilman, P., Biedenbender, S.H., Watson, M.C., Amer, S., Weltz, M., Goodrich, D., Marsett, R., 2006. Remote sensing for grassland management in the arid southwest. Rangel. Ecol. Manag. 59, 530–540.
McLean, A., Tisdale, E., 1972. Recovery rate of depleted range sites under protection from grazing. J. Range Manag. 178–184.
McSherry, M.E., Ritchie, M.E., 2013. Effects of grazing on grassland soil carbon: a global review. Glob. Chang. Biol. 19, 1347–1357. https://doi.org/10.1111/gcb.12144.
Moran, P., 1950. Notes on continuous stochastic phenomena. Biometrika 37, 17–23.
Murphy, M.A., Evans, J.S., Storfer, A., 2010. Quantifying Bufo boreas connectivity in Yellowstone National Park with landscape genetics Linked references are available on JSTOR for this article : quantifying Bufo boreas connectivity in Yellowstone National Park with landscape genetics. Ecology 91, 252–261.
Pebesma, E.J., 2004. Multivariable geostatistics in S: the gstat package. Comput. Geosci. 30, 683–691. https://doi.org/10.1016/j.cageo.2004.03.012.
Phinn, S.R., Stow, D.A., Franklin, J., Mertes, L.A.K., Michaelsen, J., 2003. Remotely sensed data for ecosystem Analyses . Combining Hierarchy Theory and Scene Models 31, 429–441. https://doi.org/10.1007/s00267-002-2837-x.
Pickup, G., Bastin, G.N., Chewings, V.H., 1994. Remote-sensing-based condition assessment for nonequilibrium rangelands under large- scale commercial grazing. Ecol. Appl. 4, 497–517.
Pineiro, G., Perelman, S., Guerschman, J.P., Jose, P.M., 2008. How to evaluate models: observed vs. predicted or predicted vs. observed? Ecol. Model. 216, 316–322. https://doi.org/10.1016/j.ecolmodel.2008.05.006.
R Development Core Team, 2016. R: A Language and Environment for Statistical Computing, vol. 0 R Found. Stat. Comput, Vienna Austria. https://doi.org/10.1038/sj.hdy.6800737. {ISBN} 3-900051-07-0.
Radtke, P.J., Boland, H.T., Scaglia, G., 2010. An evaluation of overhead laser scanning to estimate herbage removals in pasture quadrats. Agric. For. Meteorol. 150, 1523–1528. https://doi.org/10.1016/j.agrformet.2010.07.010.
Rahman, A.F., Gamon, J.A., Sims, D.A., Schmidts, M., 2003. Optimum pixel size for hyperspectral studies of ecosystem function in southern California chaparral and grassland. Remote Sens. Environ. 84, 192–207. https://doi.org/10.1016/S0034-4257(02)00107-4.
Robel, R.I., Briggs, J.N., Dayton, A.D., Hulbert, L.C., 1970. Relationships between visual obstruction measurements and weight of grassland vegetation relationships between visual obstruction measurements and weight of grassland vegetation. J. Range Manag. 23, 295–297.
Sadoti, G., Pollock, M.G., Vierling, K.T., Albright, T.P., Strand, E.K., 2014. Variogram models reveal habitat gradients predicting patterns of territory occupancy and nest survival among vesper sparrows. Wildl. Biol. 20, 97–107. https://doi.org/10.2981/wlb.13056.
Sankey, T.T., Sankey, J.B., Weber, K.T., Montagne, C., 2009. Geospatial assessment of grazing regime shifts and sociopolitical changes in a Mongolian rangeland. Rangel. Ecol. Manag. 62, 522–530. https://doi.org/10.2111/.1/REM-D-09-00014.1.
Sayre, N.F., deBuys, W., Bestelmeyer, B.T., Havstad, K.M., 2012. "The range problem" after a century of rangeland science: new research themes for altered landscapes. Rangel. Ecol. Manag. 65, 545–552. https://doi.org/10.2111/REM-D-11-00113.1.
Sayre, N.F., McAllister, R.R., Bestelmeyer, B.T., Moritz, M., Turner, M.D., 2013. Earth Stewardship of rangelands: coping with ecological, economic, and political marginality. Front. Ecol. Environ. 11, 348–354. https://doi.org/10.1890/120333.
Scarth, P., Trevithick, R., 2017. Management effects on ground cover "Clumpiness": scaling from field to Sentinel-2 cover estimates. Int. Arch. Photogramm. Remote Sens. Spat. Inf. Sci. - ISPRS Arch. 42, 183–188. https://doi.org/10.5194/isprs-archives-XLII-3-W2-183-2017.
Schaefer, M.T., Lamb, D.W., 2016. A Combination of Plant NDVI and LiDAR Measurements Improve the Estimation of Pasture Biomass in Tall Fescue (Festuca Arundinacea. https://doi.org/10.3390/rs8020109.
Strahler, A.H., Woodcock, C.E., Smith, J.a., 1986. On the nature of models in remote sensing. Remote Sens. Environ. 20, 121–139. https://doi.org/10.1016/0034-4257(86)90018-0.
Tisdale, E.W., 1982. In: Grasslands of Western North America, (A. C. N. ed).
Todd, S.W., Hoffer, R.M., Milchunas, D.G., 1998. Biomass estimation on grazed and ungrazed rangelands using spectral indices. Int. J. Remote Sens. 19, 427–438.
Townsend, D.E., Fuhlendorf, S.D., 2010. Evaluating relationships between spatial heterogeneity and the biotic and abiotic environments. Am. Midl. Nat. 163, 351–365. https://doi.org/10.1674/0003-0031-163.2.351.
Turner, W., Spector, S., Gardiner, N., Fladeland, M., Sterling, E., Steininger, M., 2003. Remote sensing for biodiversity science and conservation. Trends Ecol. Evol. 18, 306–314. https://doi.org/10.1016/S0169-5347(03)00070-3.
Vierling, K.T., Vierling, L. a, Gould, W. a, Martinuzzi, S., Clawges, R.M., 2008. Lidar: shedding new light on habitat characterization and modeling. Front. Ecol. Environ. 6, 90–98. https://doi.org/10.1890/070001.
Virk, R., Mitchell, S.W., 2015. Effect of different grazing intensities on the spatial-temporal variability in above-ground live plant biomass in north American mixed grasslands. Can. J. Remote Sens. 40, 423–439. https://doi.org/10.1080/07038992.2014.1009882.
Wang, D., Xin, X., Shao, Q., Brolly, M., Zhu, Z., Chen, J., 2017. Modeling aboveground biomass in Hulunber grassland ecosystem by using unmanned aerial vehicle discrete lidar. Sensors 17, 1–19. https://doi.org/10.3390/s17010180.
Wang, R., Gamon, J.A., 2019. Remote sensing of terrestrial plant biodiversity. Remote Sens. Environ. 231, 111218. https://doi.org/10.1016/j.rse.2019.111218.
West, N.E., 2003. Theoretical underpinnings of rangeland monitoring. Arid Land Res. Manag. 17 333–246.
Western, A.W., Blöschl, G., Grayson, R.B., 1998. Geostatistical characterisation of soil moisture patterns in the Tarrawarra catchment. J. Hydrol 205, 20–37. https://doi.org/10.1016/S0022-1694(97)00142-X.
Wiens, J., Sutter, R., Anderson, M., Blanchard, J., Barnett, A., Aguilar-Amuchastegui, N., Avery, C., Laine, S., 2009. Selecting and conserving lands for biodiversity: the role of remote sensing. Remote Sens. Environ. 113, 1370–1381. https://doi.org/10.1016/j.rse.2008.06.020.
Wiens, J.A., 1989. Spatial scaling in ecology. Funct. Ecol. 3, 385–397.
Wijesingha, J., Moeckel, T., Hensgen, F., Wachendorf, M., 2019. Evaluation of 3D point cloud-based models for the prediction of grassland biomass. Int. J. Appl. Earth Obs. Geoinf. 78, 352–359. https://doi.org/10.1016/j.jag.2018.10.006.
Woodcock, C.E., Strahler, A.H., 1987. The factor of scale in. Remote Sens. 332, 311–332.
Woodcock, C.E., Strahler, A.H., Jupp, D.L., 1988. The use of variograms in remote Sensing : I . Scene models and simulated images. Remote Sens. Environ. 25, 323–348. https://doi.org/10.1016/0034-4257(88)90108-3.
Xu, D., Guo, X., Li, Z., Yang, X., Yin, H., 2014. Measuring the dead component of mixed grassland with Landsat imagery. Remote Sens. Environ. 142, 33–43. https://doi.org/10.1016/j.rse.2013.11.017.
Zlinszky, A., Deák, B., Kania, A., Schroiff, A., Pfeifer, N., 2015. Mapping natura 2000 habitat conservation status in a pannonic salt steppe with airborne laser scanning. Remote Sens. 7, 2991–3019. https://doi.org/10.3390/rs70302991.
Zlinszky, A., Schroiff, A., Kania, A., Deák, B., Mücke, W., Vári, Á., Székely, B., Pfeifer, N., 2014. Categorizing grassland vegetation with full-waveform airborne laser scanning: a feasibility study for detecting natura 2000 habitat types. Remote Sens. 6, 8056–8087. https://doi.org/10.3390/rs6098056.